

PROCEEDINGS OF SPIE

[SPIDigitalLibrary.org/conference-proceedings-of-spie](https://spiedigitallibrary.org/conference-proceedings-of-spie)

Low And Moderate Resolution Spectroscopy With An Rca Charge-Coupled Device (CCD)

Oke, J.

J. B. Oke, "Low And Moderate Resolution Spectroscopy With An Rca Charge-Coupled Device (CCD)," Proc. SPIE 0290, Solid-State Imagers for Astronomy, (1 January 1981); doi: 10.1117/12.965835

SPIE.

Event: Solid State Imagers for Astronomy, 1981, Cambridge, United States

Low and moderate resolution spectroscopy with an RCA charge-coupled device (CCD)

J. B. Oke

Palomar Observatory, California Institute of Technology, 105-24, Pasadena, California 91125

Abstract

An RCA buried channel thinned 320 x 512 CCD has recently been put into operation as the detector on the blue side of a new double spectrograph used at the Cassegrain focus of the Hale 5.08-meter telescope. The chip is used in a vacuum dewar at a temperature of -132°C . The electronics are essentially the same as those used by Westphal and Gunn for the Texas Instruments 800 x 800 CCD's. The readout noise over most of the chip is 46 electrons per pixel, but on one side of the device there are columns with readout noise three times as high as this. The dark current is approximately 85 electrons per pixel per hour and for most purposes can be neglected.

When used in a spectroscopic mode with an $f/1.5$ beam the CCD shows interference patterns with an amplitude of 5 to 20 percent. This pattern occurs most clearly above 5000 Å. It appears to be stable and can be removed by using standard flat-field exposures. At signal levels of a few hundred electrons there are some charge transfer problems. The quantum efficiency between 4000 and 6500 Å is very high and the efficiency at 3260 Å is about 20 percent of that at 4200 Å. Above 6500 Å the sensitivity begins to drop steadily.

Introduction

A 320 x 512 buried channel thinned RCA CCD has recently been put into operation at Palomar Observatory. The device is primarily used on a new low-to-moderate resolution double spectrograph which is attached to the Hale 5.08-meter telescope. The CCD is at the focus of a folded Schmidt $f/1.5$ camera which has a focal length of 225 mm.

The chip is mounted in a vacuum dewar and is operated at a controlled temperature of -132°C . The electronics for the RCA CCD were made as nearly as possible the same as those currently being used for 800 x 800 TI CCD's by Westphal and the Space Telescope Wide-Field Camera group. The first off-chip amplifier and some drive electronics are mounted in the dewar while four P-C cards, in two small "saddle-bags" are mounted on the outside of the dewar.

A CCD controller has also been built which provides the interface between the camera electronics and a PDP 11/40 computer. The controller stores and relays one readout line on request from the computer. Housekeeping parameters such as chip temperature, etc. are also available through the controller. Since the electronics for the RCA and TI CCD's are nearly identical, the controller can be used with either kind of camera.

Pictures read from the CCD by the computer are stored on a 78 Mbyte disk and also read out on a magnetic tape. Pictures can be flattened and displayed on a TV monitor immediately.

Readout noise and erase frames

We will refer to a picture read out without exposure to light as an erase frame. This frame consists of a preset DC level, readout noise, and any peculiarities which the chip may have. Part of one such frame is shown in Figure 1. A plot of the average readout level in the fast readout 320 pixel direction is shown in Figure 2. The vertical scale is in DN where 1 DN = 6 electrons. In most of the picture the readout noise is approximately 46 el./pixel. There are, however, obvious horizontal lines where the readout noise is considerably higher. These columns are a function only of the position in the 320 pixel readout line, and not the 512 direction. These odd columns, which are spaced approximately every 16 pixels, change somewhat when the delay time between readouts of lines of data is changed, but they are always present. The noise in these columns can be three times that of the other quiet columns. In practice the spectrum is put on the half of the chip where these odd columns are least visible.

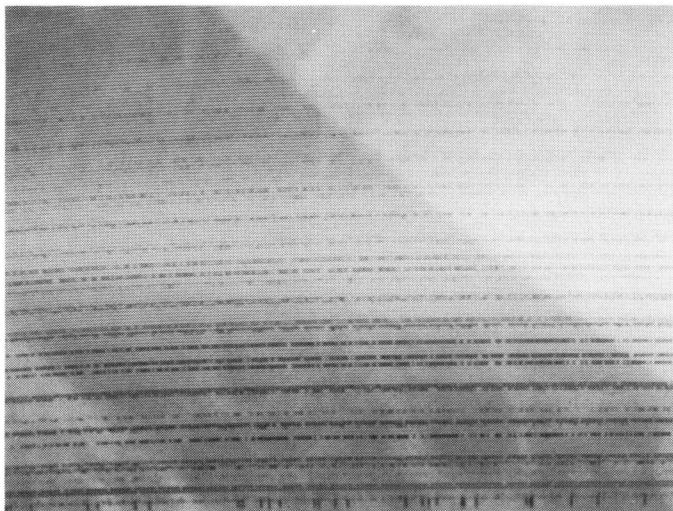


Figure 1. Part of an erase frame.

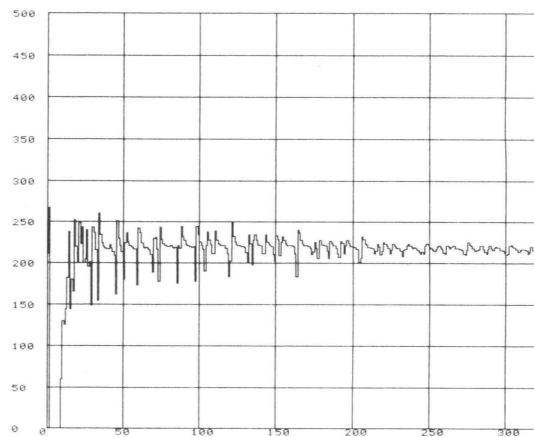


Figure 2. Average erase readout level.

Dark current

At a temperature of -132°C , the dark current should be almost negligible. One hour exposures give an average dark current of 85 electrons per hour per pixel. There is some variability over the surface of the chip. For exposures of less than an hour or two dark current can be neglected. A typical one hour exposure shows about 15 hot spots. The majority of these are presumably caused by cosmic rays since their positions do not repeat from one exposure to another.

Quantum efficiency

Because we are using the CCD in a spectrometer we have not yet measured its quantum efficiency absolutely since the efficiency of the spectrometer also must be known. If we put in estimates of the telescope and spectrometer efficiencies we find quantum efficiencies of 20 to 30 percent between 4000 and 6000 \AA . On a similar basis the quantum efficiencies of bialkali and S20 photocathodes turn out to be approximately 10 percent at 4500 \AA . Since such calculations always are uncertain by about a factor two, the quantum efficiency specifications provided by RCA appear to be realistic.

Our particular CCD has a peak quantum efficiency near 6500 \AA ; it decreases steadily to the red of 6500 \AA but still has some sensitivity at 10830 \AA . Thus the far red sensitivity of this chip is much less than that of the TI chips. We have been able to obtain satisfactory stellar spectra down to 3200 \AA where the earth's atmosphere becomes opaque. We estimate that the quantum efficiency at 3260 \AA is about 20 percent of that at 4200 \AA .

As soon as the CCD camera can be adapted for direct imaging, the quantum efficiency will be measured absolutely using narrow band filters and out-of-focus standard star images.

Flat fields and optical interference effects

This RCA CCD, used in a spectrophotometric mode, shows the usual optical interference effects caused by the near-monochromatic light and variations in thickness of the thinned CCD. These patterns are seen both in the blue and red with the prominence of the pattern being quite different at different wavelengths. Figure 3 shows a picture of the balance factors used for a spectrum which stretches from 5100 \AA on the left to 4000 \AA on the right. A plot along one horizontal row of pixels is shown in Figure 4. The slow undulations are a function of the way in which the balance factors are derived and not a consequence of irregular quantum efficiency. In this particular frame the amplitude of the fringes is approximately 5 percent. At redder wavelengths, particularly at higher spectral resolution, the fringe amplitude can be as high as 10 to 20 percent.

As long as slits which have widths comparable to or smaller than one pixel are used, the interference effects can be removed accurately using flat field spectra generated by incandescent lamps. Figure 4 shows the signal along a single row of pixels in a standard star spectrum (5400 \AA is on the left, 4300 \AA on the right). The same spectrum after flattening is shown in Figure 6. Clearly the interference effects have disappeared. Even in regions where the fringe amplitude is 20 percent there is no serious difficulty in removing the

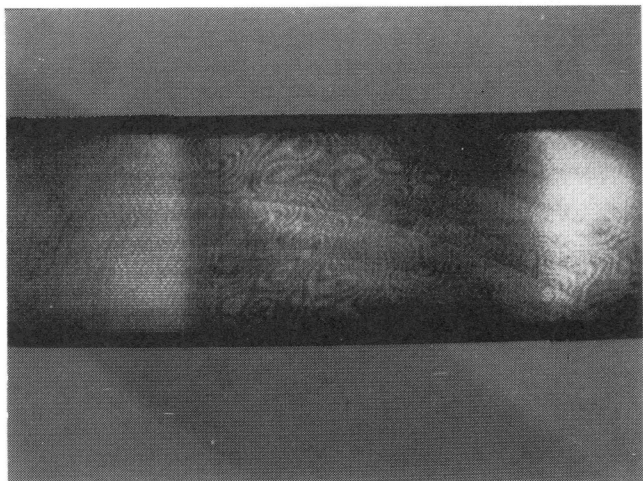


Figure 3. Balance factors over the central part of the CCD.

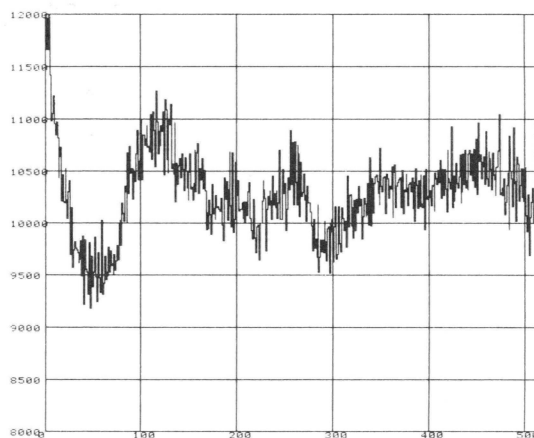


Figure 4. Balance factors along one horizontal row in Figure 3.

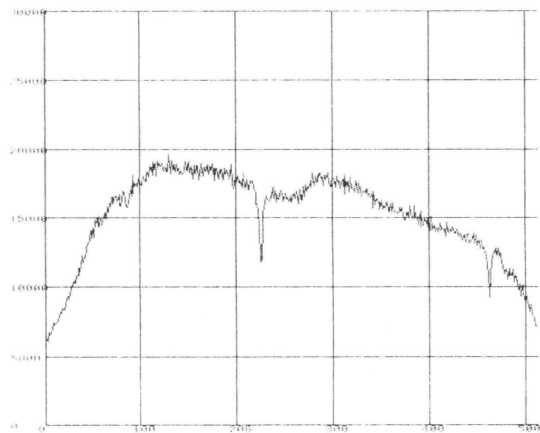


Figure 5. Standard star spectrum along one row of pixels before flattening. The wavelength range is 5400 Å to 4300 Å.

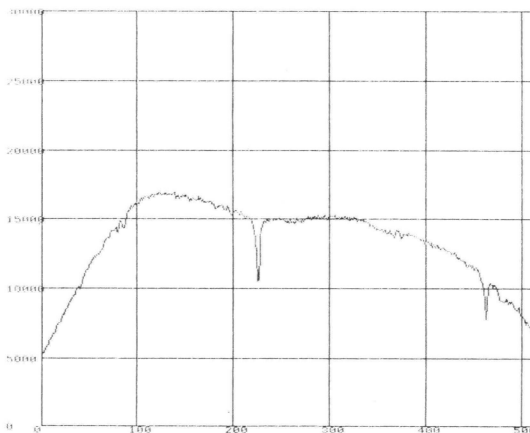


Figure 6. The same spectrum as Figure 5 but after flattening.

interference effects. An example is shown in Figure 7 which is an unflattened standard star spectrum ranging from 8700 to 4600 Å; the flattened spectrum is in Figure 8.

There are modes of operation, however, where it is difficult or impossible to remove the interference effects. Spectrophotometric observations made with large apertures, i.e. 7 to 10 arcseconds diameter, are possible with our new double spectrograph and present serious problems. Such observations produce large round monochromatic images of the night sky emission lines superposed on a smoother "continuous" spectrum. There appears to be no easy way to remove the interference effects with flat-field calibration exposures.

Charge transfer problems

At low signal levels, corresponding to a few hundred electrons per pixel, charge is smeared out over a few pixels behind the bright one in the fast readout direction. It is possible to alter the effect by changing drive voltages; it is not, however possible to eliminate it. One possible solution is to illuminate the chip uniformly with a light source to build up the charge above some threshold. This increases the effective readout noise by a small amount. Since the effect is perpendicular to the dispersion in our spectrometer, we have not yet incorporated such a light source. There appear to be no charge transfer problems along the 512 pixel direction.

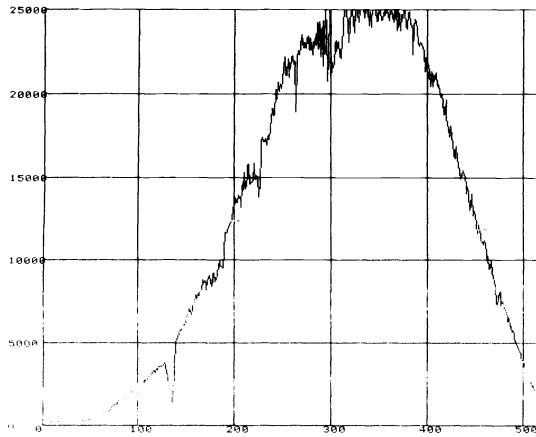


Figure 7. The same as Figure 5, but in the red from 8700 Å to 4600 Å.

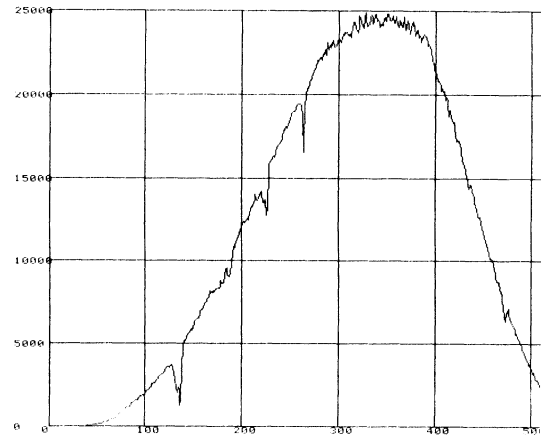


Figure 8. The same as Figure 7 after flattening.

Spectra of astronomical objects

The spectra shown below have been processed by (1) removing the erase level, (2) multiplying the frame by balance factors, (3) summing the pixels with object signals, and (4) subtracting the sky background. Wavelengths from comparison spectra have not yet been added, atmospheric extinction has not yet been removed, and the correction to absolute flux derived from the standard star data has not been applied.

Figure 9 shows a spectrum of the standard subdwarf star HD19445. The spectrum goes from approximately 8700 Å on the left to 4600 Å on the right. The prominent features are the atmospheric A and B bands, and H α and H β in the stellar spectrum. A blue spectrum of a similar standard star HD84937 is shown in Figure 10. The spectrum goes from 5100 to 4000 Å. The lines are H β , H γ and H δ .

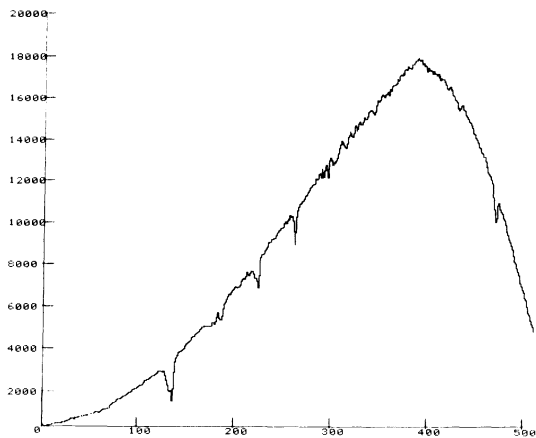


Figure 9. Spectrum of the subdwarf star HD19445 from 8700 to 4600 Å.

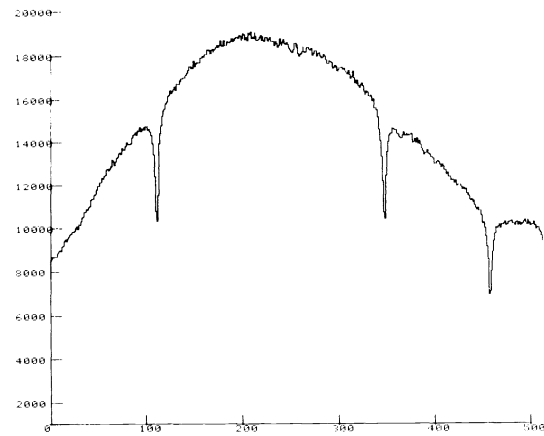


Figure 10. Spectrum of the subdwarf star HD84937 from 5100 Å to 4000 Å.

A red spectrum (8700 to 4600 Å) of the variable Seyfert galaxy 3C 120 is shown in Figure 11. The scale is 8.0 Å per pixel. The exposure time was 1000 s. The strongest emission line is H α while the three lines on the right are [OIII] 4959 and 5007 and H β . A blue spectrum of the Seyfert galaxy NGC 4151 is shown in Figure 12. The exposure was 500 s. and the scale is 2.15 Å pixel⁻¹. From the left the strong emission lines are H β , λ 4686 of HeII, λ 4363 of [OIII], H γ , H δ , λ 4068 and λ 4076 of [SII], λ 3968 and λ 3869 of [NeIII].

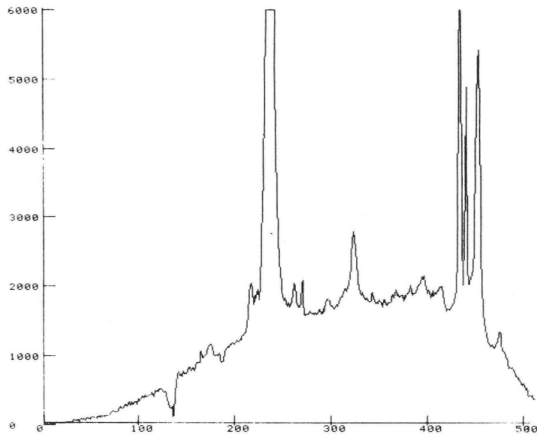


Figure 11. A spectrum from 8100 Å to 4600 Å of 3C 120.

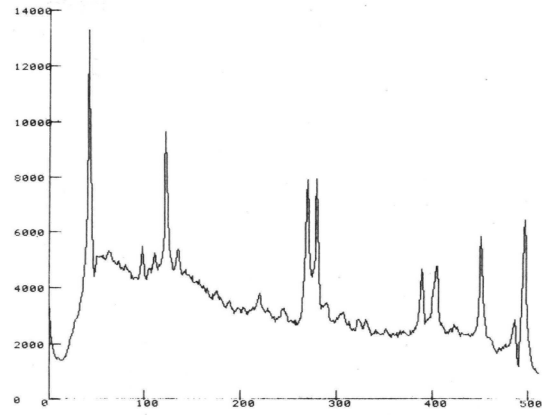


Figure 12. A blue spectrum of the Seyfert galaxy NGC 4151.

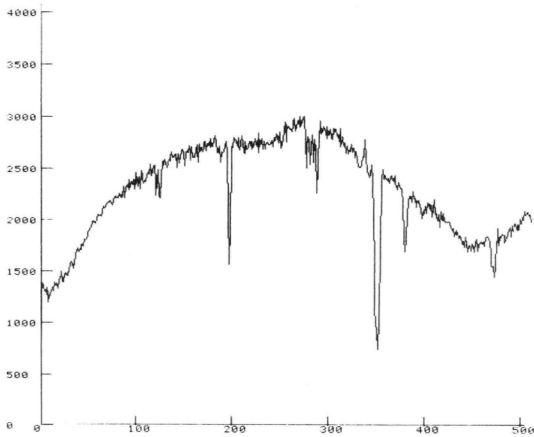


Figure 13. A blue spectrum of the quasar B2 1225+31.

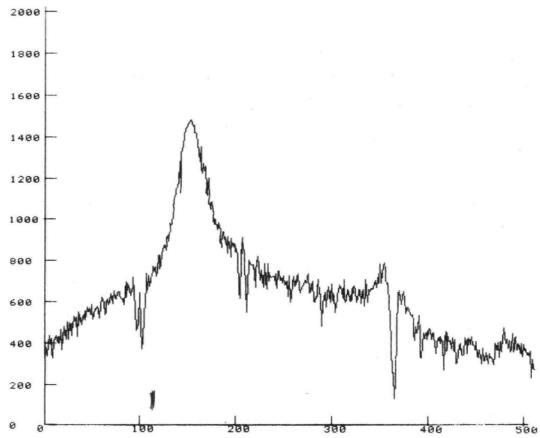


Figure 14. A blue spectrum of the quasar 1331+170.

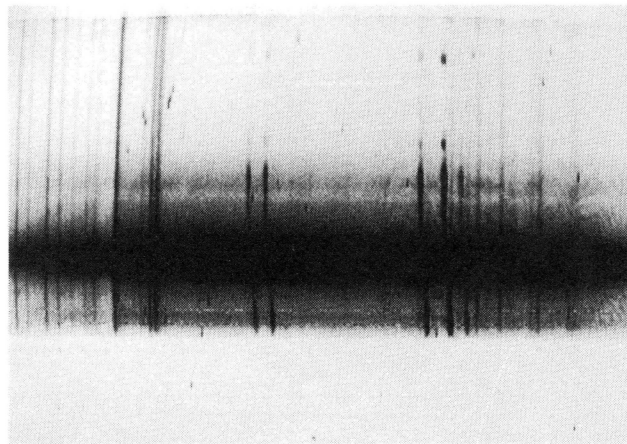


Figure 15. Spectrum of NGC 4569.

A blue spectrum of the quasar B2 1225+31 is shown in Figure 13. The broad emission near the center is $\lambda 1400$ of SiIV while $L\alpha$ is on the extreme right side. The absorption lines correspond to several lower redshift systems. Figure 14 shows a spectrum of the quasar 1331+170. The very strong emission line is $\lambda 1550$ of CIV while the weaker emission line with a strong absorption line at the center is $\lambda 1400$ of SiIV.

Figure 15 is a long slit spectrum of NGC 4569, an Sb galaxy in the Virgo cluster. An analysis of the emission line displacements yields a rotation curve for the galaxy. An accuracy of about 4 km s^{-1} is possible from these spectra.

Acknowledgements

Work on the CCD camera and software were supported by the National Aeronautics and Space Administration through grant NGL 05-002-134 and by the National Science Foundation through grant AST 7824842. The author wishes to thank B. Zimmerman and T. Boroson for providing the software for both data acquisition and reduction, F. H. Harris and G. Pauls for electronic design and construction, and J. E. Gunn and J. A. Westphal for generous assistance and advice.